Caenorhabditis elegans Inositol 5-Phosphatase Homolog Negatively Regulates Inositol 1,4,5-Triphosphate Signaling in Ovulation ⓥ

Yen Kim Bui and Paul W. Sternberg*

Howard Hughes Medical Institute and Division of Biology, California Institute of Technology, Pasadena, California 91125

Ovulation in *Caenorhabditis elegans* requires inositol 1,4,5-triphosphate (IP_3) signaling activated by the epidermal growth factor (EGF)-receptor homolog LET-23. We generated a deletion mutant of a type I 5-phosphatase, *ipp-5*, and found a novel ovulation phenotype whereby the spermatheca hyperextends to engulf two oocytes per ovulation cycle. The temporal and spatial expression of IPP-5 is consistent with its proposed inhibition of IP_3 signaling in the adult spermatheca. *ipp-5* acts downstream of *let-23*, and interacts with *let-23*–mediated IP_3 signaling pathway genes. We infer that IPP-5 negatively regulates IP_3 signaling to ensure proper spermathecal contraction.

INTRODUCTION

A crucial aspect of signal transduction is understanding how regulatory mechanisms ensure a precise biological response to pathway activation. Activation of receptor tyrosine kinases (RTK) stimulates phospholipase C to hydrolyze phosphatidyl 4,5-bisphosphate to inositol 1,4,5 triphosphate (IP_3), which binds the tetrameric IP_3 receptor to mobilize intracellular calcium (Majerus, 1992; Berridge, 1993). IP_3 signaling mediates many cellular processes (Berridge and Irvine, 1989; Berridge, 1993). Mechanisms for attenuating and terminating signaling, such as provided by proteins that metabolize IP_3, are critical in maintaining fine control of the physiological responses dependent on IP_3-mediated calcium release. Thus, it is important to understand negative regulation of IP_3 signaling.

Previous biochemical studies have shown how IP_3 is produced (Berridge and Irvine, 1984), how it is metabolized (Majerus, 1992), and how it releases intracellular calcium (Berridge, 1995; Bootman and Berridge, 1995; Clapham, 1995); however, they have not directly addressed IP_3 function in an intact metazoan. Two enzymes have been bio-

chemically identified that participate in IP_3 metabolism and potentially regulate signaling output: IP_3 kinase (IP_3K) and inositol polyphosphatase 5-phosphatase (Majerus, 1992; Drayer *et al.*, 1996). 5-Phosphatases lower IP_3 levels by dephosphorylating the 5′-phosphate, and they vary in substrate specificity (Mitchell *et al.*, 1996; Erneux *et al.*, 1998). Type I 5-phosphatases are the most active in hydrolyzing IP_3 and IP_4 (Verjans *et al.*, 1992; Laxminaryayan *et al.*, 1993). Thus, they likely play a larger role in regulating cellular levels of IP_3 than do the type II phosphatases, which additionally hydrolyze the 5′-phosphoinositols, phosphatidyl inositol 4,5-bisphosphate and phosphatidyl inositol 3,4,5-trisphosphate (Mitchell *et al.*, 1996). The distinct functional roles of various type II 5-phosphatase family members have been demonstrated by examining targeted deletions of mammalian type II 5-phosphatases in mice (Helgason *et al.*, 1998; Janne *et al.*, 1998; Cremona *et al.*, 1999) and targeted disruption of type II 5-phosphatases in yeast (Stolz *et al.*, 1996). The functional consequence of removing type I 5-phosphatase activity in vivo is unknown.

Ovulation in *Caenorhabditis elegans* hermaphrodites provides a genetic system to study the regulation of IP_3 signaling in vivo. *C. elegans* mutants defective in IP_3K, known as *lfe-2*, have no obvious ovulation defect, suggesting that an alternate pathway to metabolize IP_3 and inhibit signaling exists. Here, we report the characterization of the gene, *ipp-5*, that encodes the *C. elegans* type I 5-phosphatase. We demonstrate that it acts downstream of the LET-23 RTK, based on epistasis analyses. We present, for the first time, in vivo characterization of a type I 5-phosphatase in an intact animal by describing ovulation defects of a deletion mutant *ipp-5(sy605)* in *C. elegans*, and we place the negative regulatory function of a type I 5-phosphatase in a behavioral context.

* Corresponding author. E-mail address: pws@caltech.edu.
ⓥ Online version of this article contains video material. Online version available at www.molbiolcell.org.
  Abbreviations used: EGF, epidermal growth factor; gf, gain-of-function; GFP, green fluorescent protein; IP_3, inositol 1,4,5 triphosphate; IP_3K, IP_3 3-kinase; IP_3R, IP_3 receptor; ORF, open reading frame; PCR, polymerase chain reaction; rf, reduction-of-function; RTK, receptor tyrosine kinases

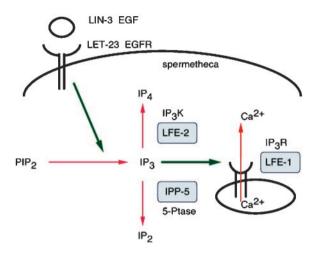**Figure 1.** IP$_3$-mediated ovulation pathway. Ovulation is dependent on an IP$_3$-mediated pathway that is activated by LIN-3 EGF and LET-23 EGFR, which likely stimulates hydrolysis of PIP$_2$ into IP$_3$. LFE-1 encodes an IP$_3$R homolog, which plays a known role in releasing intracellular calcium. LFE-2 encodes an IP$_3$K that phosphorylates IP$_3$ into IP$_4$ (Clandinin *et al.*, 1998). IPP-5 encodes a 5-phosphatase (5-Ptase), which likely dephosphorylates IP$_3$ into IP$_2$.

MATERIALS AND METHODS

Genetic Strains

Standard methods for maintaining *C. elegans* at 20°C were used. EMS (50 mM) was used as a mutagen (Brenner, 1974). Bristol strain N2 was used as the wild type. The following alleles were used: LG1, *unc-57(ad592)*, *lfe-2(sy326)*; LGII, *unc-4(e120)*, *let-23(sy10)*, *let-23(sa62)*; LGIV, *unc24(e138)*, *lin-3(n1058)*, *lfe-1/itr-1(sy290)*, *dec-4(sa73)*; LGX, *lon-2(e678)*, *unc-6(e78)*, *ipp-5(sy605)*. *szT1[lon-2(e678)]* is a reciprocal I;X translocation balancer. *mnC1[dpy-10(e128) unc-52(e444)]* is a rearrangement balancer chromosome on LGII. *DnT1[nT1[unc(n745dm)let]* is a reciprocal IV;V translocation balancer (strains are from Brenner, 1974; Ferguson and Horvitz, 1985; Fodor and Deak, 1985; Aroian *et al.*, 1991; Iwasaki *et al.*, 1995; Katz *et al.*, 1996; Clandinin *et al.*, 1998).

Brood Assay

L4 larvae hermaphrodites were serially transferred to fresh plates every 12 h for 4 d at 20°C, and progeny were counted 2 d after eggs hatched.

Polymerase Chain Reaction (PCR)

A PCR-based strategy was used to screen a library of 245, 000 EMS mutagenized N2 haploid genomes for a targeted deletion in *ipp-5* (using the method of G. Moulder and R. Barstead, personal communication; http://pcmc41.ouhsc.edu/Knockout/). The deletion removes 242 base pairs (bp) upstream of the ATG through 25 bp of exon 3. The following primers were used to detect the deletion in lysates: Round I, JC43 (5′ TGCCTTGCACAAGATTATCG) and JC46 (5′ CTCTCCTTCTTCCACCAA); Round II, JC30 (5′CAGCCCAT-GAGTCACTACTTCC) and JC68 (5′ CTAGGAGGTTTTGAATTTT-GACCTG). Wild-type animals amplify a 1300-bp product, whereas *ipp-5* deletion mutants amplify a 480-bp product. The deletion mutant was backcrossed seven times to *lon-2 unc-6*. The presence of the deletion in double mutants was verified by PCR using primer pairs JC68 and BY4 (5′ CGTTTTCCTTTGACGAAAGCTCGG) in Round II to distinguish homozygotes (700-bp band) from heterozygotes (700

bp, 1600-bp band). The mutants were scored by Nomarski video recordings of ovulation.

Microscopy and Image Processing

Worms were anesthetized for 30 min in a solution of M9 with 0.1% tricaine and 0.01% tetramisole (Sigma, St. Louis, Missouri) before recording (McCarter *et al.*, 1999). Animals were mounted on 5% agarose pads with 20 μl of anesthetic, covered with an 18-mm glass coverslip, and the edges of the coverslip were sealed with Vaseline. Observations were made at 20°–23°C. Animals were mounted on an Axioscope (Zeiss, Thornwood, New York) and recorded under Nomarski optics (Plan 100 objective) for no more than 4 h. The microscope was connected to a CCD72 DAGE-MTI (Michigan City, Indiana) charged-coupled device video camera module and VCR. Images were recorded on VHS tape in real time. While under anesthetic, oocyte maturation, and sheath and spermathecal activity at ovulation proceed, whereas pharyngeal pumping and egg laying cease (McCarter *et al.*, 1999). Spermathecal extension distance was calculated by direct measurement of length (starting from the side of the proximal oocyte nearest the spermatheca to the point at which the spermathecal valve closes to envelop the oocytes) on the monitor during video production. Distance was calibrated on each set-up to convert centimeters on the monitor to true micrometer values using a stage micrometer. For ovulation movies, VHS video recordings were dubbed onto DVCAM digital tapes, captured as computer DV stream files via fire wire, and then the frame speed increased by 900% using the software program Final Cut Pro (Apple Computer, Cupertino, California). Video compression for Internet playback was performed using the Cleaner 5 Software Application (Autodesk/Discreet Logic Inc., Montreal, Quebec). Still-frame images (720 × 480 pixels) were grabbed from the ovulation computer-captured DV stream file (Digital Media Center, Caltech, Pasadena, California).

For fluorescent microscopy, animals were viewed with ×100 objective under a green fluorescent protein (GFP) filter. Images were collected using a digital camera (C4742–95; Hamamatsu, Middlesex, New Jersey), transferred to a computer (G3 Macintosh; Apple Computer, Cupertino, California) running Open Lab Imaging 1.7.8r3 Software (Improvision, Coventry, England, and assembled in Photoshop (Adobe Systems, Mountain View, California).

ipp-5 cDNA Sequence Analysis

A full-length cDNA, yk341d7, kindly provided by Yuji Kohara (expressed sequence tag partial sequence GenBank accession C44206), was sequenced on both strands and compared with the wild-type *ipp-5* genomic sequence from the Sequencing Consortium (The *C. elegans* Sequencing Consortium, 1998) to obtain the splicing pattern. Genefinder predicts a slightly different cDNA (WormBase WS51) than the full-length cDNA we sequenced (GenBank accession AF411588). One base pair was found missing in exon 2 in the cDNA clone yk341d7, creating a frameshift premature stop codon. Genomic DNA amplified from N2 worms was sequenced on both strands and matched the sequence provided by the Consortium, indicating the mutation in the cDNA was an artifact. The mutation was repaired using a QuikChange Site-Directed Mutagenesis kit (Stratagene, La Jolla, California), yielding mut2IP5. Sequencing confirmed the mutation was corrected and that no other artifactual mutations occurred in the cDNA.

Construction of Transgenes

Standard molecular biology techniques were used (Sambrook *et al.*, 1989). To examine the *ipp-5* expression pattern, a 2-kb sequence upstream of the ATG, including exon 1, was amplified from genomic N2 DNA (using high-fidelity LA Takara *Taq*) and cloned into the pGEM TA cloning vector and then subcloned into the GFP

expression vector pPD95.77 (A. Fire) with MluNI and Kpn sites, yielding pYB10. The entire *ipp-5* locus was amplified from N2 genomic DNA and was subcloned into pPD49.83 (A. Fire) at the Kpn/*Eco*RV site, yielding pYB8. The entire *ipp-5* genomic region was sequenced, and no extraneous mutations were found. A 2-kb sequence upstream of the start ATG codon was subcloned in place of the HS promoter at the MluNI and Kpn sites of pYB8, yielding pYB11 to test if the native promoter driving expression of the genomic *ipp-5* locus rescues the *sy605* phenotype.

Three constructs using heterologous promoters driving the *ipp-5* cDNA were generated. A 1.0-kb region upstream of ZK370.3 was amplified from pCeh (kindly provided by A. Parker) using primers SphpCeh (5′ CCCGCATGCCTGCAGTTCTCCTCTCTG CC) and KpnpCeh (5′ CCCCGGTACCAAAAAAATTAATTTTTTTGGGGGC) and was cloned into pPD49.83 (A. Fire) at the MluN and Kpn site. A *Bam*HI/Asp718 fragment containing the pCeh promoter was then subcloned into vector mut2IP5 with *Bam*HI and *Eco*RI/blunted sites, yielding pYB13. The promoter was sequenced to verify that no additional mutations occurred during amplification. We examined *dpy-5(e905) hIs29[pCeh361; pCeh363]* (kindly provided by A. Parker), which carries the pCeh::GFP transgene, and we confirmed that the pCeh promoter shows expression in the adult spermatheca and not the sheath (A. Parker, personal communication). For pYB14, the entire cDNA from mut2IP5 was subcloned into the heat shock vector pPD49.83 (A. Fire) at the Nhe/Kpn site. For pYB15, a 3-kb *nlp-8* promoter (Nathoo *et al.*, 2001), which expresses in the sheath (Anne Hart, personal communication), was amplified using primers AN46 (5′ GAAGCTTCTGACTCATGTCGC) and *Bam*HIAN49 (5′ CCGCGGATCCTGCATGCATTACTGTATTCAAAATTACGGTG) from genomic DNA and was subcloned into mut2IP5 using *Bam*HI and *Eco*RI/blunted sites. We examined the strain *him-5; lin-15(n795) rtEx22[nlp-8::GFP, lin-15(+)]* (kindly provided by A. Hart) and confirmed expression in the proximal sheath cells and not in the spermatheca (Anne Hart, personal communication).

Construction of Transgenic Strains

Transgenic strains were generated as described by Mello *et al.* (1991). To assess whether the genomic *ipp-5* locus, including the 2-kb 5′ sequence upstream of the ATG, rescues the phenotype in *sy605* animals, we injected pYB11 along with *myo-2::gfp* as a transformation marker. Rescue of *ipp-5(sy605)* was determined by scoring the ovulation phenotype of three lines under Nomarski optics and recording ovulations of transgenic *ipp-5(sy605) syEx[pYB11; myo-2::gfp]* worms. We observed one ovulation event in each gonad arm per animal. Moreover, *sy605* transgenics containing the heat shock transgene pYB14 and *myo-2::gfp* also showed rescue upon induction with a heat shock pulse of 33°C for 40 min in the young adult stage. The cosmids encompassing *ipp-5* did not show the expected restriction pattern, and thus were not used to assay for rescue. We built the transgenic strain *sy605 syEx*[pYB13; *myo-2::gfp*] to test rescue with a heterologous spermathecal promoter. Additionally, we built the transgenic strain *sy605 syEx[pYB15; myo-2::gfp]* to test rescue with a heterologous sheath promoter. The *ipp-5*::GFP fusion was injected with pRF4 [*rol-6(su1006)*] as a transformation marker in *sy605* animals or N2 animals to examine the expression pattern. Both transgenic strains show identical expression.

RESULTS

ipp-5 Encodes a Type I 5-Phosphatase Homolog

To better understand the regulation of IP$_3$ signaling, we sought to identify additional downstream genes involved in the LET-23 RTK-mediated IP$_3$ signaling pathway for ovulation in *C. elegans* (Clandinin *et al.*, 1998). Clandinin *et al.* (1998) identified *lfe-1*, an IP$_3$ receptor (IP$_3$R) homolog, and *lfe-2*, an IP$_3$K homolog, as suppressors of *lin-3(rf)* sterile ovulation defective mutants, indicating that ovulation is dependent on an evolutionary conserved IP$_3$ signaling pathway (Figure 1). Video analysis of *lfe-2* mutants shows no obvious ovulation defect (see Video 1), suggesting the inositol polyphosphate 5-phosphatase, which also metabolizes IP$_3$ in other systems, may play a critical role inhibiting signaling in *C. elegans* ovulation. The *C. elegans* genome sequence predicts an ortholog of the human type I inositol polyphosphate 5-phosphatase (CO9B8.1), which we designate *ipp-5* (The *C. elegans* Sequencing Consortium, 1998). We sequenced a full-length *ipp-5* cDNA (kindly provided by Y. Kohara) corresponding to this region, and found 11 nucleotides of an SL1 trans-spliced leader and a single open reading frame (ORF), comprising 7 exons that encode a 400-amino acid protein 42% identical to its human counterpart (Figure 2). The *C. elegans* IPP-5 lacks the well-conserved motif (GDLNYRL) present in all members of the type II 5-phosphatases, as seen in the *C. elegans* homolog, C16C2.3 (Figure 2B). However, IPP-5 contains the conserved active site motif (PAWC/TDRV/ILM) essential for enzymatic activity of all type I and type II 5-phosphatases (Communi *et al.*, 1996; Jefferson and Majerus, 1996; Majerus, 1996; Erneux *et al.*, 1998). On this basis, we classify IPP-5 as a type I phosphatase. IPP-5 lacks the C-terminal isoprenylation site CCVVQ present in members of the 5-phosphatase type I family, suggesting that it relies on another mechanism for targeting to its correct intracellular location.

ipp-5 Affects Ovulation and Fertility

To study *ipp-5* function, we isolated a deletion mutant, *ipp-5(sy605)*, in which 240 bp upstream of the start codon is deleted through 28 bp of exon 3. We examined *ipp-5(sy605)* mutant animals for defective ovulation. There are no other obvious visible defects.

In a wild-type hermaphrodite, oocytes align on the proximal–distal axis of the gonadal sheath and mature in an assembly-line manner as they proceed proximally toward the spermatheca. Typically, during ovulation, the sheath contracts and pulls the dilated spermatheca over the most proximal mature oocyte in the proximal gonad to release it from the oviduct into the spermatheca (McCarter *et al.*, 1999). Animals with defects in ovulation have a reduced brood size. For example, analysis of Nomarski ovulation videos indicate that *let-23(sa62)* RTK gain-of-function (gf) and *dec-4/itr-1* IP$_3$R reduction-of-function (rf) mutants show mechanical defects in ovulation [*dec-4(sa73)*, n = 20/20 defective ovulations; *let-23(sa62)*, n = 12/12 defective ovulations; see Videos 3 and 4] and have lower broods than wild type (mean brood 121 ± 9 [SD], see Figure 4B, [Dal Santo *et al.*, 1999]; *let-23(sa62)* mean brood 173, range 45–276, n = 24, [Katz *et al.*, 1996]). In *sa62* mutants, the spermatheca constricts abnormally and tears the ovulated oocyte, leaving the nucleus behind in the gonad. The defect in *sa73* mutants is more pronounced; the basal sheath contraction rate in *sa73* mutants appears reduced relative to wild type, and the spermatheca dilates and constricts continually during ovulation before it finally pinches shut, tearing the oocyte and leaving the nucleus behind. Furthermore, *lin-3(rf)* or *let-23(rf)* mutants are sterile (Aroian *et al.*, 1991) because they fail to ovulate (Clandinin *et al.*, 1998; McCarter *et al.*, 1999).

Figure 3 shows a sequential image series of a wild-type and a *sy605* hermaphrodite during ovulation (see Videos 2 and 5). The deletion mutant shows a novel ovulation phe-
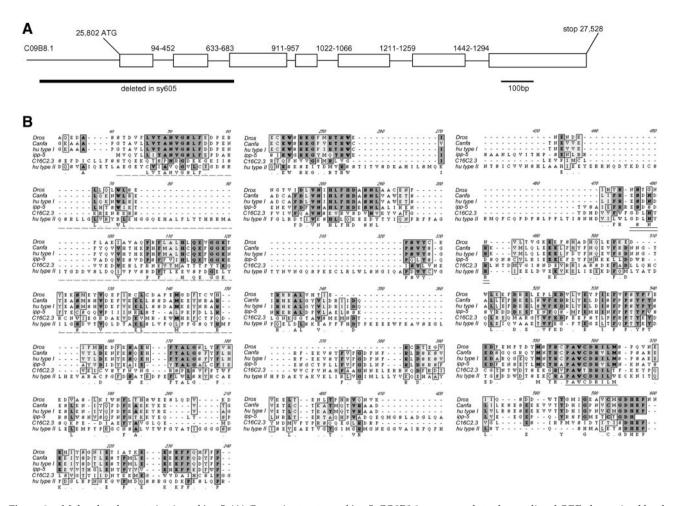
Figure 2. Molecular characterization of *ipp-5*. (A) Genomic structure of *ipp-5*. CO9B8.1 corresponds to the predicted ORF, determined by the Genefinder Program, to encode a *C. elegans* homolog of the inositol polyphosphate 5- phosphatase. Exons are shown as white boxes. The sequence is inferred from the cDNA (generously provided by Y. Kohara). The numbers above each intron indicate the base pair position relative to itself. The indicated region deleted in *sy605* spans 240 bp upstream of the start ATG codon through exon 3. (B) Protein sequence alignment of the *Drosophila,* dog, human, and *C. elegans* homologs of the type I inositol 5-phosphatase and the *C. elegans* and human homologues of the type II 5-phosphatase. A *Drosophila* homolog has not been identified genetically, but Genie has predicted an ORF (GenBank accession AAF56383) in the sequenced genome. Identical residues are darkly shaded, and conserved substitutions are lightly shaded. The signature motif present in all 5-phosphatase family members is underlined in black. The motif well conserved among all type II phosphatases is double underlined. The residues deleted in *ipp-5* are indicated by a dashed underline.

notype whereby more than one oocyte is ovulated per cycle. In these double ovulations, the spermatheca dilates and extends beyond the proximal oocyte to precociously envelop the second and in some cases the third oocyte. In *sy605*, the spermatheca extends on average 49.1 ± 11.9 μm (n = 18) compared with 33.9 ± 4.7 μm in the wild type (n = 30; p < 0.0001, Fisher's Exact test). This observation indicates that IPP-5 is required to prevent excessive spermathecal dilation and extension during ovulation.

Prior work by McCarter *et al.* (1999) suggests that ovulation is coupled to oocyte meiotic maturation. In *sy605* mutant animals, along with the proximal oocyte, the secondary oocyte is ovulated precociously, before the hallmarks of maturation are observed (McCarter *et al.*, 1999). The presence of the nucleolus and nuclear envelope in these precocious oocytes indicates they have not undergone maturation

(Figure 4). This mutant phenotype raises the possibility that there is no absolute requirement for an oocyte to have undergone maturation to be ovulated. In *ceh-18* mutants, immature oocytes are ovulated but do not appear to form zygotes (Rose *et al.*, 1997). In *sy605,* the distal oocytes ovulated before maturation are apparently not fertilized because we have seen oocytes interdigitating with fertilized multicellular eggs in the uterus (n = 9). Video analysis of the fate of the secondary oocyte (ovulated precociously) indicates fertilization and embryogenesis does not ensue, as observed in the accompanied fertilized primary oocyte (n = 11/11). Taken together, these results suggest that although meiotic maturation is not required for ovulation, it may be required for fertilization.

sy605 homozygotes have a reduced brood of 144 ± 20 (n = 25) relative to the wild-type brood of 337 ± 33 (n = 20, p <
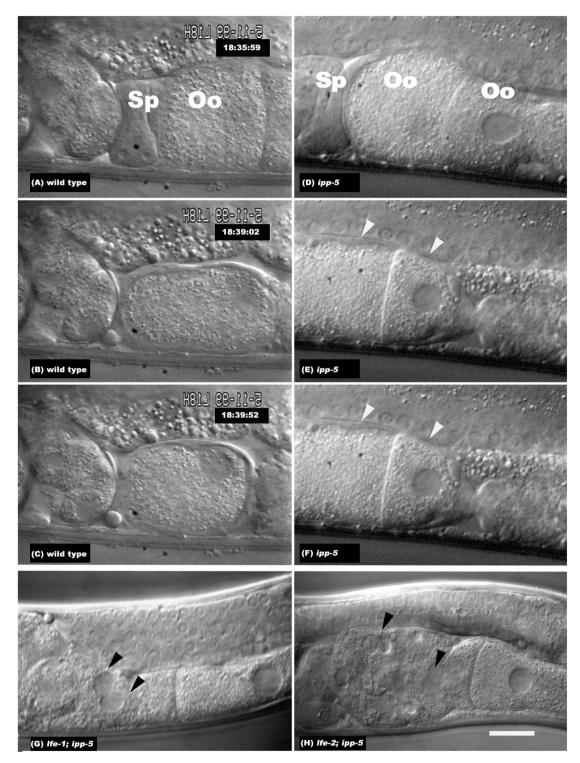
Figure 3. *ipp-5(sy 605)* effects on ovulation. Still-frame series of Nomarski photomicrographs of a hermaphrodite (A–C) wild-type and (D–F) *ipp-5* gonad during ovulation. The wild-type images have been flipped horizontally so the orientation matches that of the *ipp-5* images. The uterus is toward the left and the proximal gonad is toward the right. The *ipp-5* phenotype shows two oocytes, indicated by white arrowheads, being ovulated in the spermatheca per cycle; see Supplementary Information Videos 2 and 5. Nomarski photomicrographs of (G) *lfe-1/itr-1*; *ipp-5* and (H) *lfe-2; ipp-5*. Double mutants between *ipp-5* and *lfe-X* cause the endomitotic oocyte nuclei (Emo) phenotype, indicated by black arrowheads. "Sp" denotes the position of the spermatheca, and "Oo" denotes the oocyte. Animals were photographed using a ×100 objective and differential interference contrast optics. Scale bar, 20 μm.
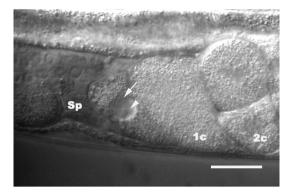
Figure 4. Fate of secondary oocyte in *ipp-5(sy605)* animals. In *sy605* mutants, the second oocyte is ovulated along with the proximal oocyte and is passed into the uterus. The secondary oocyte has not undergone maturation, as the nucleolus (arrowhead) and the nuclear envelope (arrow) are still present. The proximal oocyte that was ovulated is at the one-cell (1c) stage. A two-cell embryo is also shown (2c). Scale bar, 20 μm.

0.001; Table 1). Animals heterozygous for the deletion have a slightly reduced brood size (314 $\pm$ 36; n = 20) relative to wild type (p = 0.0437; Table 1). Heterozygotes ovulate one oocyte/cycle (n = 54) as do wild type, indicating the double ovulation phenotype is recessive.

To confirm that the deletion in the *ipp-5* locus causes the observed ovulation defect, we tested whether a transgene containing the full-length wild-type genomic *ipp-5* locus, including the 2-kb sequence upstream of the start ATG codon, could complement the defect in *sy605* transgenic animals. In *sy605* animals, the ovulation defect is fully penetrant on a per animal basis (n = 15/15 animals double ovulate); however, looking at successive ovulations in animals, we observe that every ovulation event is not mutant (49% of gonad arms ovulate one oocyte/cycle, n = 70; Table 2B). Transgenic *sy605* animals bearing the *ipp-5* genomic locus as an extrachromosomal array showed rescue in all three lines examined (Table 2A). Thus, the ovulation defect is likely the result of the deletion, which removes *ipp-5* function, because the phenotype can be rescued by adding back wild-type copies of the *ipp-5* gene. It is conceivable that the next in-frame methionine downstream of the deletion, but upstream of the catalytic domain, initiates protein synthesis producing a protein. This protein, which lacks the N-terminal region, might result in altered protein activity, and thus the deletion might result in a gf phenotype. However, we think this possibility is inconsistent with our rescue data and our genetic epistasis and interaction data in which *ipp-5(sy605)* behaves as a stronger version of *lfe-2*, which is a loss-of-function (see below). Thus, the simplest interpretation of the data is that *ipp-5(sy605)* is a loss-of-function mutation. Based on our mutant phenotype, we infer that IPP-5 likely regulates IP$_3$ signaling, which modulates spermathecal dilation/contraction.

IPP-5 Acts in the Adult Spermatheca

To investigate where *ipp-5* might function, we examined the expression of a *ipp-5*::GFP transcriptional reporter. A 2-kb fusion of 5′ sequence directed expression in the adult distal spermatheca and weakly in the proximal sheath in transgenic animals (Figure 5). This same promoter sequence driving the genomic *ipp-5* locus is sufficient to rescue the defect in *sy605* transgenic animals (Table 2A). To test whether expression in the spermatheca is sufficient for rescuing the ovulation defect, we used a heterologous spermathecal promoter (kindly provided by A. Parker) to drive expression of the *ipp-5* cDNA. We observed rescue of the ovulation defect in two transgenic *sy605* lines observed. In *sy605* animals, 51% of the gonad arms examined were mutant where more than one oocyte was ovulated per cycle, whereas 33% mutant gonad arms were observed in *sy605* animals bearing the transgene as an extrachromosomal array (p < 0.0246). In a second line, 20% of the gonad arms were mutant (p = 0.0002; Table 2B). Thus, expression of the transgene led to significantly more animals with normal ovulation, indicating that expression of *ipp-5* in the spermatheca is sufficient to rescue the ovulation defect. Although *ipp-5*::GFP expression is also detected in the vulva and isthmus of the pharynx throughout larval development and adulthood, we think it unlikely that expression in these tissues affects the spermathecal contraction behavior. Transgenic *sy605* worms injected with a transgene containing a sheath promoter (kindly provided by A. Hart) driving the *ipp-5* cDNA did not show rescue of the ovulation defect in four lines observed (Table 2B). Together with the expression data, we infer *ipp-5* likely functions within the adult spermatheca to regulate ovulation.

We did not observe expression of the *ipp-5*::GFP reporter transgene before adulthood in the spermatheca, suggesting the function of *ipp-5* is needed in the adult spermatheca for ovulation rather than for the development or specification of the sheath and spermatheca lineages, which occurs in the L4 larval stage (Kimble and Hirsh, 1979). We observed L4 stage *sy605* hermaphrodites under Nomarski optics and found that they had normal spermathecae and proximal sheath: The numbers of spermathecal cells were normal, and there was no obvious abnormality in spermathecal morphogenesis or in the proximal ovarian sheath (n = 13). To determine if expression of *ipp-5* in adult stage is sufficient for its function in ovulation, we examined whether using a heat shock promoter driving the *ipp-5* cDNA to induce expression in *sy605* adults is sufficient to rescue the ovulation defect. In two lines observed, induced expression of *ipp-5* function in adults was sufficient to rescue the double ovulation phenotype in transgenic *sy605* worms: line 1, 22% mutant gonad arms after heat shock vs. 53% mutant gonad arms in control transgenic animals with no heat shock, p = 0.0005; line 2, 26% mutant gonad arms after heat shock vs. 49% mutant gonad arms in control transgenic animals with no heat shock, p = 0.0123 (Table 2C). We conclude that IPP-5 activity is not required before the L4 larval stage for its function in ovulation. The temporal and spatial regulation of *ipp-5* is consistent with its regulatory function during adult ovulation rather than in developmental processes that secondarily affect dilation.

ipp-5 Suppresses the Sterility of **lin-3** *and* **let-23**

LIN-3 has been proposed to activate LET-23 and an IP$_3$ signaling pathway (Clandinin *et al.*, 1998) that regulates ovulation. This pathway comprises *lin-3*, *let-23*, *lfe-1*, and *lfe-2* encoding an epidermal growth factor (EGF)-like growth factor, EGFR, IP$_3$R, and IP$_3$K, respectively (Figure 1). *lin-3(rf)*

Table 1. *ipp-5(sy605)* suppresses the sterility of *lin-3(rf)* and *let-23(rf)* and synergizes with other genes in the *let-23*–mediated fertility pathway

Genotype				
other	*ipp-5*	Fertile	n	Brood
+	+/+	100%	20	337 ± 33
let-23(rf)	+/+	0%	40	0
lin-3(rf)	+/+	1.3%	76	0.2 ± 1.8
+	*sy605/sy605*	100%	25	144 ± 20
+	*sy605/+*	100%	20	314 ± 36
let-23(rf)	*sy605/sy605*	100%	21	n.d.[a]
lin-3(rf)	*sy605/sy605*	98.7%	319	28 ± 9 (n = 47)
lfe-1(gf)	+/+	100%	26	207 ± 35
lfe-2(lf)	+/+	100%	23	213 ± 34
lfe-1(gf)	*sy605/sy605*	24%	55	6.0 ± 12
lfe-2(lf)	*sy605/sy605*	0%	86	0

Fertile is defined as having greater than five offspring. Alleles used are *lin-3(n1058)*, *let-23(sy10)*, *lfe-1(sy290)* and *lfe-2(sy326)*. *unc-4(e120)* was used as a marker and *mnC1[dpy-10(e128) unc-52(e444)]* as a balancer for *let-23*, and *unc-24(e138)* was used as a marker and *DnT1[nT1[unc(n745dm)let]* as a balancer for *lin-3*. *lfe-1* was marked with *unc-24(e138)* and *lfe-2* was marked with *unc-57(ad592)*.

[a] *sy10* animals display a partially penetrant larval lethal phenotype associated with *let-23(rf)* decreases in RAS signaling, thus broods were not determined. n.d., not determined.

and *let-23(rf)* mutants are sterile, producing no progeny because they fail to ovulate. These mutants have an Emo phenotype in which the oocytes become trapped in the gonad arm and undergo multiple rounds of DNA synthesis (Clandinin *et al.*, 1998; McCarter *et al.*, 1999). A gf mutation in *lfe-1* IP$_3$R or a loss-of-function mutation in *lfe-2* IP$_3$K can

Table 2. In vivo transgenic assay for rescue of *ipp-5(sy605)* ovulation defect

ipp-5 Genotype	Transgene	Line #	Conditions	Gonad arms (1 oocyte ovulated/cycle)	Gonad arms (2 oocytes ovulated/cycle)		Gonad arms (n)
A. Rescue by genomic *ipp-5* DNA							
+				100%	0%		43
sy605				0%	100%		15
sy605	*ipp-5*	1		74%	26%	p < 0.0001	57
sy605	*ipp-5*	2		73%	27%	p < 0.0001	51
sy605	*ipp-5*	3		66%	34%	p < 0.0001	32
B. Site of action							
pCEH spermtheca promoter driving *ipp-5* cDNA is sufficient for rescue							
sy605				49%	51%		70
sy605	*pCeh::ipp-5*	23.1		67%	33%	p = 0.0246	93
sy605	*pCeh::ipp-5*	9.1		80%	20%	p = 0.0002	65
nlp-8 sheath promoter driving *ipp-5* cDNA is not sufficient for rescue							
sy605				49%	51%		70
sy605	*nlp-8::ipp-5*	4.1		47%	53%	p = 0.8685	77
sy605	*nlp-8::ipp-5*	10.1		40%	60%	p = 0.3780	60
sy605	*nlp-8::ipp-5*	1.2		35%	65%	p = 0.1930	51
sy605	*nlp-8::ipp-5*	1.1		47%	53%	p = 1.000	76
C. Heat shock-induced expression of *ipp-5* cDNA in young adults is sufficient for rescue							
sy605	*hs::ipp-5*	18.2	No HS	47%	53%		51
sy605	*hs::ipp-5*	18.2	+ HS	78%	22%	p = 0.0005	78
sy605	*hs::ipp-5*	22.1	No HS	51%	49%		53
sy605	*hs::ipp-5*	22.1	+ HS	74%	26%	p = 0.0123	66

(A) During ovulation in wild-type animals, the spermatheca envelops one oocyte. In *ipp-5(sy605)* animals, the spermatheca ovulates two and sometimes three oocytes at a time. A 2-kb sequence upstream of the ATG along with the entire genomic *ipp-5* locus rescues the phenotype when injected as a transgene in *sy605* animals (3/3 lines rescued). (B) A heterologous spermatheca promoter, pCeh (provided by Alex Parker), fused to the *ipp-5* cDNA also rescues the defect in *sy605* transgenic animals (2/2 lines rescued), whereas the *nlp-8* sheath–specific promoter (Anne Hart, personal communication) does not (0/4 lines rescued). (C) A heat shock promoter driving expression of *ipp-5* cDNA in adults rescues the ovulation defect (2/2 lines rescued). HS, heat shock.
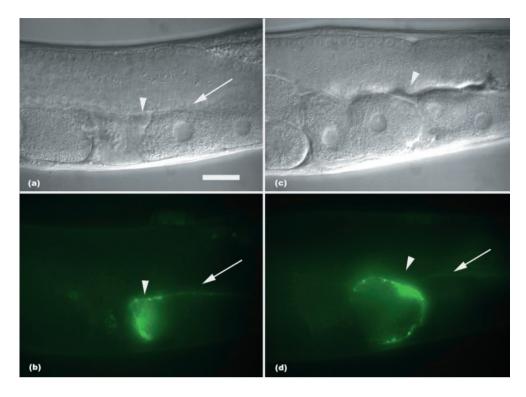
Figure 5. Expression of *ipp-5*. Nomarski photomicrographs of a transgenic worm and their corresponding GFP fluorescence photomicrographs. The white arrowhead indicates position of the distal spermatheca, and the white arrow indicates the sheath. (A and B) A worm before ovulation. (C and D) A transgenic *sy605* worm during ovulation. The arrowhead indicates the distal spermatheca enclosing two oocytes in a *sy605* transgenic animal. Strong expression is detected in the distal spermatheca, whereas faint expression is detected in the sheath. Fertilized embryos are to the left, and oocytes lining up in the proximal gonad are to the right. Scale bar, 20 μm.

bypass the requirement for wild-type levels of LET-23 activity: *lin-3(rf); lfe* or *let-23(rf); lfe* double mutants are fertile (Clandinin *et al.*, 1998). We tested whether the *C. elegans* IPP-5 functions downstream of LET-23 RTK and can suppress the sterility of either *lin-3(rf)* or *let-23(rf)*. *lin-3(n1058)*, which affects vulva induction and fertility, has an average brood size of 0.2 ± 1.8 (n = 76). In contrast, *lin-3(n1058); ipp-5(sy605)* double mutants are 98.7% fertile (n = 319), having an average brood size of 28 ± 9, n = 47 (Table 1); an allele of *lin-3*, *n378*, which affects only vulva induction (causing a vulvaless phenotype where the animals are unable to lay eggs), has an average brood size of 72 ± 11, n = 17 (Clandinin *et al.*, 1998). Similarly, *ipp-5* suppresses *let-23(rf)*, as 100% of *let-23(sy10); ipp-5(sy605)* double mutants are fertile (n = 21; Table 1). Because *sy605* can suppress the sterile defect of *lin-3* as well as *let-23*, we conclude that *ipp-5* functions downstream of *lin-3* and *let-23* to mediate ovulation.

ipp-5 Synergizes with Other Genes in the let-23–mediated Fertility Pathway

We next examined genetic interactions of *ipp-5* with known components of the fertility pathway. *lfe-1/itr-1(gf)* or *lfe-2(lf)* single mutants have a slightly reduced brood size and ovulate normally (Clandinin *et al.*, 1998). *ipp-5* synergizes with either *lfe-1(gf)* or *lfe-2(lf)* to produce a synthetic sterile Emo phenotype (Figure 3) similar to that observed in *lfe-1(gf); lfe-2(lf)* double mutants (Clandinin *et al.*, 1998) where the spermatheca fails to dilate sufficiently. *lfe-1(sy290); ipp-5* double mutants have an average brood of 6 ± 12 (n = 55) compared with *lfe-1(sy290)*, which has an average of 207 ± 35(n = 26). *lfe-2(sy326)* has a brood of 213 ± 34 (n = 23), whereas *lfe-2(sy326); ipp-5* double mutants are sterile, pro-

ducing no progeny (n = 86; Table 1). The data indicate that *ipp-5* interacts with both *lfe-1/itr-1* and *lfe-2* and that it likely functions in the adult spermatheca to regulate the fertility pathway during ovulation. Consistent with this hypothesis, all three proteins are expressed in the adult spermatheca (Clandinin *et al.*, 1998; Dal Santo *et al.*, 1999; Gower *et al.*, 2001).

ipp-5(sy605) exhibits a semidominant synergistic effect in a sensitized background. Analysis of ovulation videos show that although *sy605/+* heterozygotes and *lfe-1* or *lfe-2* single mutants do not double ovulate, *sy605* heterozygotes that are also homozygous for *lfe-2* double ovulate and are fertile (n = 17). Similarly, *sy605* heterozygotes that are also homozygous for *lfe-1* are fertile and double ovulate (n = 10). *sy605* synergizes with *lfe-1* and *lfe-2* mutations in a dose-sensitive manner, because removing two copies of *ipp-5* has more severe affects than removing a single copy. The Emo phenotype observed in the *lin-3(rf)* or *let-23 (rf)* single mutant and double mutant *ipp-5; lfe-1* or *ipp-5; lfe-2* suggests that IP$_3$ signaling levels are critical for normal hermaphrodite ovulation and fertility. From our study on *ipp-5* mutant phenotypes, we infer that IPP-5 inhibits IP$_3$ signaling after activation to ensure that ovulation occurs properly.

To further examine the affects of varying IP$_3$ signaling on ovulation, we examined double mutants of *ipp-5* with a gf allele of *let-23(sa62)* RTK (Katz *et al.*, 1996). *sa62* animals have a reduced brood, which may in part be attributed to the sickness of the homozygotes (average brood 173, range 24–276 progeny, n = 24; Katz *et al.*, 1996), and an ovulation defect where the spermathecal valve contracts prematurely, closing and tearing the oocyte as it enters (n = 12; see Video 4). *ipp-5* also synergizes with *sa62*, causing a further reduc-

tion in brood size (average brood 7; range 0–27 progeny; n = 31). In these double mutants, the spermatheca extends beyond the proximal oocyte to the second oocyte, but it then retracts and has problems ovulating the proximal oocyte, eventually causing an Emo phenotype (n = 8). Precise control of IP$_3$ levels appears to be crucial in vivo for proper spermathecal dilation. Thus, both insufficient and excessive IP$_3$ signaling cause defective ovulation.

IPP-5 and LFE-2 Have Different Roles in Regulating IP3 Signaling

Both the 5-phosphatase and 3-kinase metabolize IP$_3$; however, their respective contributions in negatively regulating IP$_3$ signaling are unclear. Clandinin *et al.* (1998) showed that *lfe-2(sy326)* mutation disrupts kinase activity because it failed to phosphorylate IP$_3$ in an in vitro kinase assay. The point mutation in *lfe-2* and the deletion in *ipp-5* are probably loss-of-function mutations. We examined the ovulation phenotype of both these alleles by Nomarski video analysis (see Videos 1 and 5). Although *lfe-2(lf)* mutants display a reduced brood size, video analysis shows no obvious defects in ovulation (n = 22), unlike *ipp-5(sy605)*. Strikingly, these genes, both of which likely regulate IP$_3$ levels, have qualitatively different loss-of-function phenotypes. We infer that IPP-5 and LFE-2 are both critical for ovulation, but act differently to regulate it. We observe no effect with misexpression of IPP-5 in wild-type worms (unpublished observations); however, misexpression of LFE-2 using a heat shock promoter causes the spermatheca to relax inappropriately (Clandinin *et al.*, 1998). The existence of multiple proteins that differentially inhibit IP$_3$ signaling highlight the importance of maintaining fine control of IP$_3$ signaling in ovulation.

DISCUSSION

In an attempt to better understand how IP$_3$ signaling downstream of the LET-23 RTK pathway affects ovulation and fertility, we have generated and characterized a deletion mutant of the *C. elegans* type I inositol polyphosphate 5-phosphatase. *ipp-5(sy605)* homozygous mutants have reduced fertility and a novel ovulation phenotype whereby the spermatheca dilates and extends abnormally. Epistasis analyses place *ipp-5* downstream of *let-23*. Two mutant loci have previously been identified that can bypass LET-23 RTK function, *let-23* fertility effectors, *lfe-1(gf)/itr-1*, an IP$_3$R homolog, a positive effector, and *lfe-2(lf)*, an IP$_3$K, a negative effector (Clandinin *et al.*, 1998). *ipp-5(sy605)* enhances *lfe-1(gf)* and *lfe-2(lf)* mutants, causing sterility. Our transgenic rescue data (Table 2) and reporter GFP expression data (Figure 5) are consistent with IPP-5 directly controlling contraction and dilation behavior in the adult spermatheca (Figure 1).

Contributions of the 5-Phosphatase and IP$_3$K and Negative Regulation of IP$_3$ Signaling

We observed that the *C. elegans* 5-phosphatase deletion mutant, *ipp-5(sy605),* and the IP$_3$K mutant, *lfe-2(lf)*, have qualitatively different ovulation phenotypes. The double ovulation phenotype of *ipp-5* probably results from increased IP$_3$ signaling upon removing IPP-5 function. Consistent with this, cell lines that stably underexpress a type I 5-phosphatase have a sustained 2.6-fold elevation in IP$_3$, leading to

enhanced intracellular calcium oscillations and cellular transformation (Speed *et al.*, 1996, 1999; Speed and Mitchell, 2000). By contrast, *lfe-2(lf)* shows no noticeable ovulation defect in *C. elegans*. We infer that eliminating activity of either gene allows IP$_3$ to accumulate to different levels, resulting in the two distinct phenotypes and suggesting that they have distinct negative regulatory roles within the context of ovulation. Studies of IP$_3$ metabolism in *Xenopus* oocytes indicate that at low [IP$_3$] and high [Ca^{2+}], IP$_3$ is metabolized predominantly by IP$_3$K, whereas as [IP$_3$] increases, the 5-phosphatase degrades progressively more IP$_3$, irrespective of the [Ca^{2+}] (Sims *et al.*, 1996). Multiple enzymes that metabolize IP$_3$ imply that tight regulation of IP$_3$ is essential for ensuring proper spermathecal dilation/relaxation during ovulation. In *C. elegans*, elevated IP$_3$ signaling affects spermathecal dilation, and IPP-5 is critical for inhibiting signaling for contraction.

Ovulation Is Regulated by IP$_3$ Signaling Levels

Cell culture studies have shown that the mammalian 5-phosphatase and IP$_3$K metabolize IP$_3$ into either IP$_2$ or IP$_4$, respectively (Irvine *et al.*, 1986; Berridge and Irvine, 1989). Simultaneously removing *ipp-5* activity and *lfe-2* activity should create a situation where IP$_3$ accumulates and exerts negative feedback inhibition, which blocks further ovulation.

We interpret the effects on spermathecal dilation in the *lfe-2; ipp-5* mutant as being mediated through either too low or excessively high levels of IP$_3$ signaling. Moreover, a double mutant with *ipp-5* and *sa62*, a gf allele of *let-23* RTK (Katz *et al.*, 1996) that has hyperactive signaling, also shows the same ovulation defect, further demonstrating the inhibitory effects of excessive IP$_3$ signaling. Cell culture studies have shown that EGF stimulates IP$_3$ production and a rise in intracellular calcium (Hepler *et al.*, 1987). An activating mutation in LET-23 RTK likely results in higher levels of second messenger IP$_3$ production. We presume that the cooperative effect of removing IPP-5 in the gf LET-23 mutant dramatically increases IP$_3$ signaling, which prevents ovulation causing the Emo phenotype.

Examining the spermatheca in these mutants allows us to see a more direct physiological effect of perturbing IP$_3$ signaling in vivo. There appears to be a biphasic phenotypic effect on the extent of spermathecal dilation and extension with increasing levels of IP$_3$ signaling in *C. elegans*. In *lin-3(rf)* and *let-23(rf)* mutants with reduced EGF signaling, IP$_3$ signaling is not sufficient for the spermatheca to dilate. In *ipp-5* mutants where IP$_3$ signaling is higher, the spermatheca dilates and extends farther than in the wild type to ovulate the proximal mature oocyte along with the secondary distal oocyte, which has not undergone meiotic maturation. One explanation for this observation is that in *sy605*, the proximal oocyte, which has undergone meiotic maturation, triggers the spermatheca to dilate. The secondary distal oocyte is passively ovulated precociously, as a consequence of the spermatheca extension beyond the proximal oocyte due to increased IP$_3$ signaling.

Further elevations in IP$_3$ signaling in various double mutants prevent spermatheca dilation. IP$_3$ positively effects gating of IP$_3$R, but has also been shown along with calcium to exert negative feedback, which may explain this phenotype (Berridge, 1993; Ehrlich and Watras, 1988; Besproz-

vanny *et al.*, 1991). Multiple layers of regulating intracellular calcium release allows fine control of many cellular processes.

LET-23 RTK-induced activation of IP_3 signaling, which promotes spermatheca dilation likely through its effect on calcium release, is reminiscent of arterial smooth muscle relaxation and arterial dilation by calcium sparks (Nelson *et al.*, 1995). The structural architecture of the myoepithelial sheath and spermatheca resemble smooth muscle. Longitudinal interdigitated thick and thin filaments make up the sheath. Actin stains the spermatheca, revealing circumferentially arranged fibers (Strome, 1986) that may undergo peristaltic vasoconstrictive and dilatory behavior like that of epithelial smooth muscle. The tension from the contracting sheath pulls the dilated spermatheca over the proximal oocyte during ovulation (McCarter *et al.*, 1999). Decreases in IP_3 signaling may trigger contraction and closure of the distal spermatheca valve so that only one oocyte is enveloped. A peristaltic wave of contraction may carry the oocyte from the distal spermatheca valve through the proximal spermathecal valve into the uterus.

Ovulation is a regulated behavior requiring coordination of the epithelial smooth muscle-like spermatheca and sheath. Animals with defective ovulation have reduced fertility, thus proper regulation of ovulation is important for normal fertility. During ovulation, we propose IPP-5 is necessary to prevent spermathecal hyperextension by negatively regulating IP_3 signaling downstream of RTK, thereby ensuring proper spermathecal dilation and contraction behavior.

ACKNOWLEDGMENTS

REFERENCES

Aroian, R., and Sternberg, P. (1991). Multiple functions of *let-23*, a *Caenorhabditis elegans* receptor tyrosine kinase gene product required for vulva induction. Genetics *128*, 251–267.

Berridge, M.J. (1993). Inositol triphosphate and calcium signaling. Nature *361*, 315–325.

Berridge, M.J. (1995). Calcium signaling and cell proliferation. Bioessays *17*, 491–500.

Berridge, M.J., and Irvine, R.E. (1984). Inositol triphosphate, a novel second messenger in cellular signal transduction. Nature *31*, 315–321.

Berridge, M.J., and Irvine, R.E. (1989). Inositol phosphates and cell signaling. Nature *341*, 197–205.

Besprozvanny, I., Waras, J., and Ehrlich, B.E. (1991). Bell-shaped calcium response curves on $Ins(1,4,5)P_3$ and calcium-gated channels from endoplasmic reticulum of cerebellum. Nature *351*, 751–754.

Bootman, M.D., and Berridge, J.M. (1995). The elemental principles of calcium signaling. Cell *83*, 675–678.

Brenner, S. (1974). The genetics of *Caenorhabditis elegans*. Genetics *77*, 71–94.

The *C. elegans* Sequencing Consortium. (1998). Genome sequence of the nematode *C. elegans*: A platform for investigating biology. Science *282*, 2012–2018.

Clandinin, T.R., DeModena, J.A., and Sternberg, P.W. (1998). Inositol triphosphate mediates a ras-independent response to LET-23 receptor tyrosine kinase activation in *C. elegans*. Cell *92*, 523–533.

Clapham, D.E. (1995). Calcium signaling. Cell *80*, 259–268.

Communi, D., Lecocq, R., and Erneux, C. (1996). Arginine 343 and 350 are two active residues involved in substrate binding by human type I D-myo-inositol 1,4,5,-trisphosphate 5-phosphatase. J. Biol. Chem. *271*, 11676–11683.

Cremona, O., Di Paolo, G., Wenk, M.R., Luthi, A., Kim, W.T., Takei, K., Daniell, L., Nemoto, Y., Shears, S.B., Flavell, R.A., McCormick, D.A., and De Camilli, P. (1999). Essential role of phosphoinositide metabolism in synaptic vesicle recycling. Cell *99*, 179–188.

Dal Santo, P., Logan, M.A., Chisholm, A.D., and Jorgensen, E.M. (1999). The inositol triphosphate receptor regulates a 50-second behavioral rhythm in *C. elegans*. Cell *98*, 757–767.

Drayer, A.L., Pesesse, X., De Smedt, F., Communi, D., Moreau, C., and Erneux, C. (1996). The family of inositol and phosphatidyl polyphosphate 5-phosphatasaes. Biochem. Soc. Trans. *24*, 1001–1005.

Ehrlich, B.E., and Watras, J. (1988). Inositol 1,4,5-trisphosphate activates a channel from smooth muscle sarcoplasmic reticulum. Nature *336*, 583–586.

Erneux, C., Govaerts, C., Communi, D., and Pesesse, X. (1998). The diversity and possible functions of the inositol polyphosphate 5-phosphatases. Biochim. Biophys. Acta *1436*, 185–199.

Ferguson, E.L., and Horvitz, H.R. (1985). Identification and characterization of 22 genes that affect the vulval cell lineages of the nematode *C. elegans*. Genetics *110*, 17–72.

Fodor, A., and Deak, P. (1985). The isolation and genetic analysis of a *C. elegans* translocation (*szT1*) strain bearing an X-chromosome balancer. J. Genet. *64*, 143–157.

Gower, N.J.D., Temple, G.R., Schein, J.E., Marra, M.A., Walker, D.S., and Baylis, H.A. (2001). Dissection of the promoter region of the inositol 1,4,5-triphosphate receptor gene, itr-1, in *C. elegans*: A molecular basis for cell-specific expression of IP3R isoforms. J. Mol. Biol. *306*, 145–157.

Helgason, C.D., Damen, J.E., Rosten, P., Grewal, R., Sorensen, P., Chappel, S.M., Borowski, A., Jirik, F., Krystal, G., and Humphries, R.K. (1998). Targeted disruption of SHIP leads to hemopoietic perturbations, lung pathology, and a shortened life span. Genes Dev. *12*, 1610–1620.

Hepler, J.R., Nakahata, N., Lovenberg, T.W., DiGuiseppi, J., Herman, B., Earp, H.S., and Harden, T.K. (1987). Epidermal growth factor stimulates the rapid accumulation of inositol (1,4,5) triphosphate and a rise in cytosolic calcium mobilized from intracellular stores in A431 cells. J. Biol. Chem. *262*, 2951–2956.

Irvine, R.F., Letcher, A.J., Heslop, J.P., and Berridge, M.J. (1986). The inositol tris/tetrakisphosphate pathway: demonstration of Ins (1,4,5) P_3 3-kinase activity in animal tissues. Nature *320*, 631–634.

Iwasaki, K., Liu, D.W.C., and Thomas, J.H. (1995). Genes that control a temperature-compensated ultradian clock in *Caenorhabditis elegans*. Proc. Natl. Acad. Sci. USA *92*, 10317–10321.

Janne P.A., Suchy S.F., Bernard D., MacDonald M., Crawley J., Grinberg A., Wynshaw-Boris A., Westphal H., Nussbaum R.L.

(1998). Functional overlap between murine Inpp5b and Ocrl1 may explain why deficiency of the murine ortholog for O.C.R.L1 does not cause Lowe syndrome in mice. J. Clin. Invest. *101*, 2042–2053.

Jefferson, A.B., and Majerus, P.W. (1996) Mutation of the conserved domains of two inositol polyphosphate 5-phosphatases. Biochem. J. *35*, 7890–7894.

Katz, W.S., Lesa, G.M., Yannoukakos, D., Clandinin, T.R., Schlessinger, J., and Sternberg, P.W. (1996). A point mutation in the extracellular domain activates LET-23, the *Caenorhabditis elegans* epidermal growth factor receptor homolog. Mol. Cell. Biol. *16*, 529–537.

Kimble, J., and Hirsh, D. (1979). Postembryonic cell lineages of the hermaphrodite and male gonads in *Caenorhabditis elegans.* Dev. Biol. *70*, 396–417.

Laxminaryayan, K.M., Matzaris, M., Speed, C.J., and Mitchell, C.A. (1993). Purification and characterization of a 43-kDa membrane-associated inositol polyphosphate 5-phosphatase from human placenta. J. Biol. Chem. *268*, 4968–4974.

Majerus, P.W. (1992). Inositol phosphate biochemistry. Annu. Rev. Biochem. *61*, 225–250.

Majerus, P.W. (1996). Inositols do it all. Genes Dev. *10*, 1051–1053.

McCarter, J., Bartlett, B., Dang, T., and Schedl, T. (1999). On the control of oocyte meiotic maturation and ovulation in *Caenorhabditis elegans*. Dev. Biol. *205*, 111–128.

Mello, C.C., Kramer, J.M., Stinchocomb, F., and Ambros, V. (1991). Efficient gene transfer in *C. elegans* extrachromosomal maintenance and integration of transforming sequences. EMBO J. *10*, 3959–3970.

Mitchell, C.A., Brown, S., Campell, J.K., Munday, A.D., and Speed, C.J. (1996). Regulation of second messengers by the inositol polyphosphate 5-phosphatases. Biochem. Soc. Trans. *24*, 994–1000.

Nathoo, A.N., Moeller, R.A., Westlund, B.A., and Hart, A.C. (2001). Identification of neuropeptide-like protein gene families in *Caenorhabditis elegans* and other species. Proc. Natl. Acad. Sci. USA *98(24)*, 14000–14005.

Nelson, M.T., Cheng, H., Rubart, M., Santana, L.F., Bonev, A.D., Knot, H.J., and Lederer, W.J. (1995). Relaxation of arterial smooth muscle by calcium sparks. Science *270*, 633–637.

Rose, K.L., Winfrey, V.P., Hoffman, L.H., Hall, D.H., Furuta, T., and Greenstein, D. (1997). The POU gene *ceh-18* promotes gonadal sheath cell differentiation and function required for meiotic maturation and ovulation in *Caenorhabditis elegans*. Dev. Biol. *192(1)*, 59–77.

Sambrook, J., Fristch, E.F., and Maniatis, T. (1989). Molecular Cloning: A Laboratory Manual, 2nd ed., Cold Spring Harbor, NY: Cold Spring Harbor Laboratory Press.

Sims, C.E., and Allbritton, N.L. (1998). Metabolism of inositol 1,4,5-triphosphate and inositol 1,3,4,5-tetrakisphosphate by the oocytes of *Xenopus laevis*. J. Biol. Chem. *273*, 4052–4058.

Speed, C.J., Little, P.J., Hayman, J.A., and Mitchell, C.A. (1996). Underexpression of the 43-kDa inositol polyphosphate 5-phosphatase is associated with cellular transformation. EMBO J. *15*, 4852–4861.

Speed, C.J., and Mitchell, C.A. (2000). Sustained elevation in inositol 1,4,5-triphosphate results in inhibition of phosphatidylinositol transfer protein activity and chronic depletion of the agonist sensitive phosphoinositide pool. J. Cell Sci. *113*, 2631–2636.

Speed, C.J., Naylon, C.B., Little, P.J., and Mitchell, C.A. (1999). Underexpression of the 43-kDa inositol polyphosphate 5-phosphatase is associated with spontaneous calcium oscillations and enhanced responses following endothelin-1 stimulation. J. Cell Sci. *112*, 669–679.

Stolz, L.E., Huynh, C.V., Thorner, J., York, J.D. (1998). Identification and characterization of an essential family of inositol polyphosphate 5-phosphatases (INP51, INP52, and INP53 gene products) in the yeast *Saccharomyces cerevisiae*. Genetics *148*, 1715–1729.

Strome, S. (1986). Fluorescence visualization of the distribution of microfilaments in gonads and early embryos of the nematode *C. elegans*. J. Cell Biol. *103*, 2241–2252.

Verjans, B., Lecocq, R., Moreau, C., and Erneux, C. (1992). Purification of bovine brain inositol-1,4,5-trisphosphate 5-phosphatase. Eur. J. Biochem. *204*, 1083–1087.